JOC The Journal of Organic Chemistry

Article

pubs.acs.org/joc

Insights into the Unexpected Chemoselectivity for the N-Heterocyclic Carbene-Catalyzed Annulation Reaction of Allenals with Chalcones

Yan Qiao,[‡] Donghui Wei,*[,†] and Junbiao Chang*[,†]

[†]The College of Chemistry and Molecular Engineering and [‡]Department of Pathophysiology, School of Basic Medical Sciences, Zhengzhou University, Zhengzhou, Henan 450001, China

Supporting Information

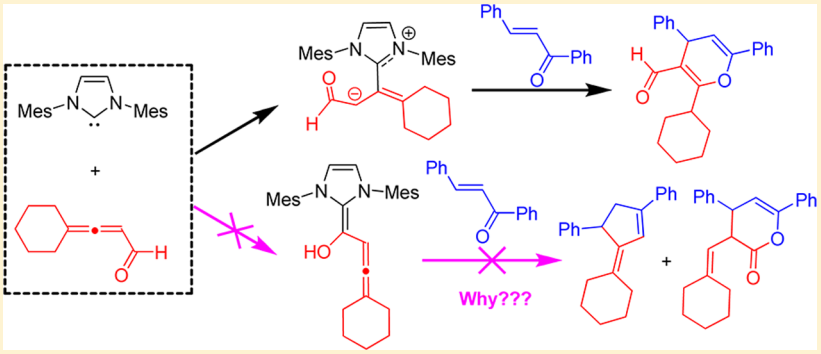

ABSTRACT: Lewis base N-heterocyclic carbene (NHC)-catalyzed annulation is the subject of extensive interest in synthetic chemistry, but the reaction mechanisms, especially the unexpected chemoselectivity of some of these reactions, are poorly understood. In this work, a systematic theoretical calculation has been performed on NHC-catalyzed annulation between allenals and chalcone. Multiple possible reaction pathways (A–E) leading to three different products have been characterized. The calculated results reveal that NHC is more likely to initiate the reaction by nucleophilic attack on the center carbon atom of the allene group but not the carbonyl carbon atom in allenals leading to the Breslow intermediate, which is remarkably different from the other NHC-catalyzed annulations of unsaturated aldehydes with chalcones. The computed energy profiles demonstrate that the most energetically favorable pathway (A) results in polysubstituted pyranyl aldehydes, which reasonably explains the observed chemoselectivity in the experiment. The observed chemoselectivity is demonstrated to be thermodynamically but not kinetically controlled, and the stability of the Breslow intermediate is the key for the possibility of homoenolate pathway D and enolate pathway E. This work can improve our understanding of the multiple competing pathways for NHC-catalyzed annulation reactions of unsaturated aldehydes with chalcones and provide valuable insights for predicting the chemoselectivity for this kind of reaction.

INTRODUCTION

In recent years, N-heterocyclic carbenes (NHCs) have been applied as the efficient organocatalyst in various carbon–carbon and carbon–heteroatom bond-forming reactions.[1−6] An attractive feature of Lewis base NHCs, as powerful organocatalysts, is their ability to catalyze the polarity reversal of various carbonyl compounds such as ketenes, saturated aldehydes, and unsaturated aldehydes. For example, the complexation of NHC and saturated aldehyde would lead to the formation of an enamine-like Breslow intermediate and thus invert the innate reactivity of aldehydes (that is, "umpolung"), i.e., with the normally electrophilic carbonyl carbon acting as a transient nucleophile (Scheme 1a). The transient nucleophile is an acyl anion equivalent and can then participate in many reactions (such as Benzoin condensation and Stetter reactions).[7,8] When the substrates are enals, i.e., α,β-unsaturated aldehydes, they do not show a similar reactivity, which is due to the more favorable homoenolate reactivity compared to that of their saturated aldehyde counterparts.[9,10] As shown in Scheme 1b, once the Breslow intermediate is formed, the β-carbon atom but not the carbonyl carbon atom would subsequently initiate the nucleophilic attack on the electrophilic reagent. Interestingly, protonation of the β-carbon of homoenolate equivalents can allow for the formation of enolate equivalents (shown in Scheme 1b).[11] By now, NHC-catalyzed reactions of enals with aldehydes,[10] imines, 1,2-diones,[12,13] cyclic 1,2-dicarbonyl compounds,[14] tropone,[15] chalcones,[16−18] and aryl nitroalkenes[19] have been extensively explored and utilized to synthesize many important natural compounds. While multiple reactive intermediates may be present in the reaction systems, the use of identical substrates may allow for the formation of different products. For example, NHC-catalyzed annulations of enals with chalcones selectively giving access to cyclopentene or enolate-type lactone compounds under the different experimental conditions have been realized by the Chi group (Scheme 1c).[20]

Received: May 31, 2015
Published: August 13, 2015

DOI: 10.1021/acs.joc.5b01222
J. Org. Chem. 2015, 80, 8619–8630

Scheme 1. (a) Formation of Acyl Anion Equivalents, (b) Formation of Homoenolate Equivalents or Enolate Equivalents, and (c) Homoenolate Pathway and Enolate Pathway

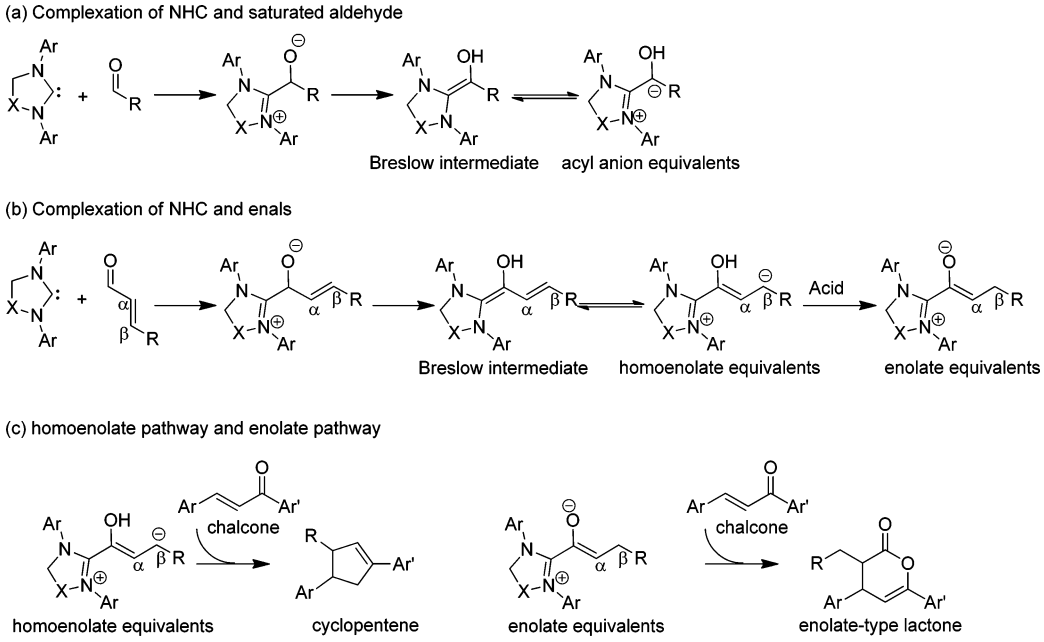

Scheme 2. NHC-Promoted Annulation Reaction of Allenals with Chalcones

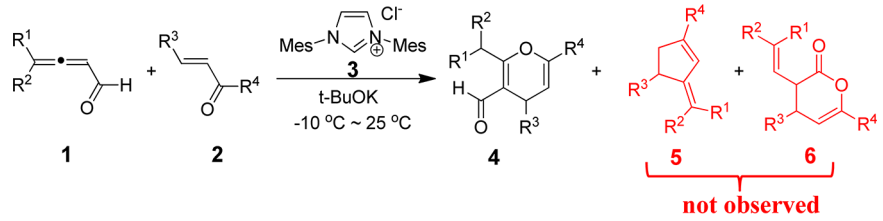

Scheme 3. Three Possible Reaction Pathways for the Formation of P1 Proposed by Ma et al.

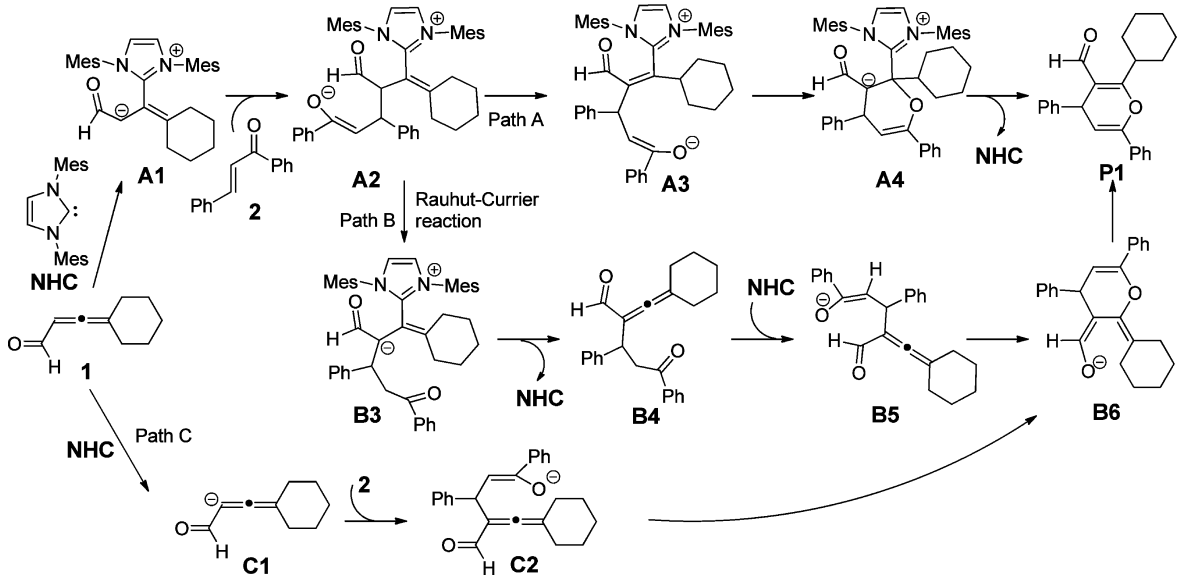

Allenals **1** are special unsaturated aldehydes. Ma et al. recently exploited their reaction with chalcones **2** catalyzed by NHC **3**, unexpectedly obtaining the polysubstituted pyranyl aldehydes **4** in good yield but not cyclopentenes **5** or enolate-type lactone products **6** (depicted in Scheme 2).[21] The reaction provides an easy method for synthesizing pyranyl aldehydes, which enriches the pyran family and provides more opportunities for efficient synthesis of natural products. However, why the reaction does not produce cyclopentenes **5** or enolate-type lactone products **6** remains ambiguous.

DOI: 10.1021/acs.joc.5b01222
J. Org. Chem. 2015, 80, 8619−8630

Scheme 4. Speculated Homoenolate Pathway D and Enolate Pathway E

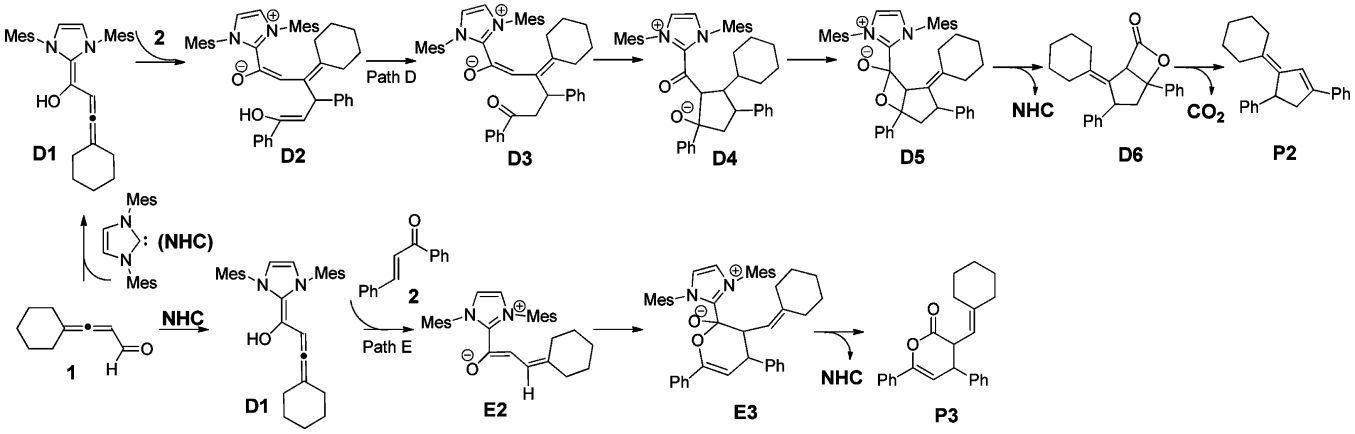

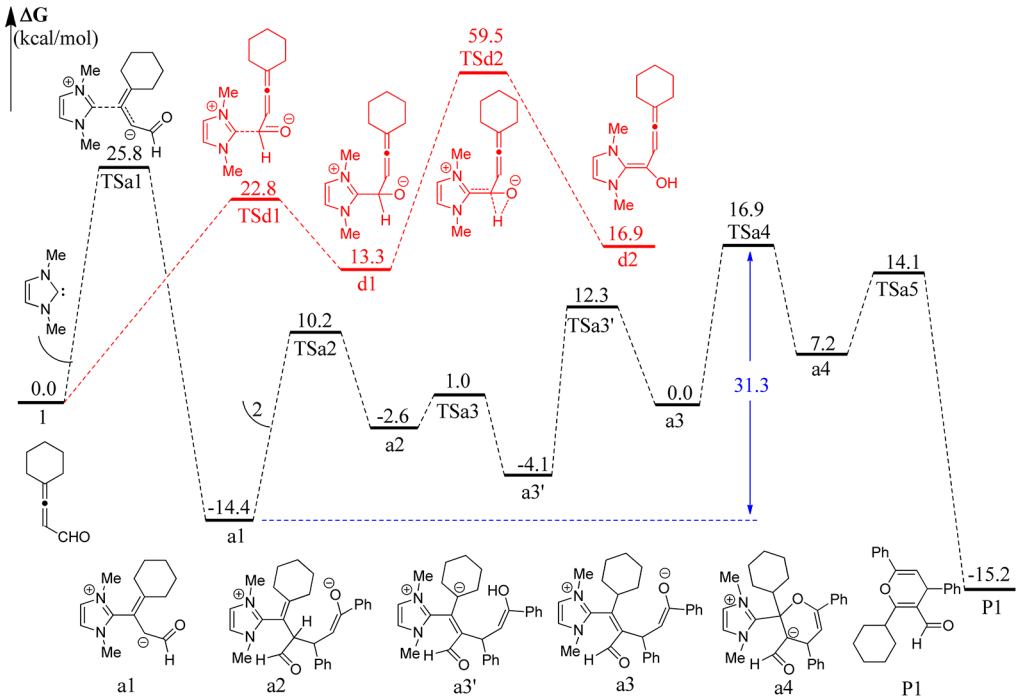

Figure 1. Summary of the computational results from Yang's work.

In the experimental report, Ma et al. speculated three possible pathways (depicted in Scheme 3). In pathway A, the NHC may attack the center carbon atom of allenals **1** leading to intermediate **A1**, which subsequently undergoes 1,4-addition with chalcone **2**, affording enolate anion intermediate **A2**. Then, intermediate **A2** would isomerize into intermediate **A3** followed by intramolecular cycloaddition and elimination of the NHC catalyst, giving final product **P1**. In pathway B, intermediate **A2** does not go through isomerization to **A3** but instead undergoes a Rauhut−Currier-type reaction to give intermediate **B3**, which would eliminate the NHC catalyst to form intermediate **B4**. Then, the regenerated NHC would abstract the α-hydrogen of **B4** to give intermediate **B5**. Finally, enolic intermediate **B5** would undergo an intramolecular cyclization to give intermediate **B6**, which is subsequently protonated with IMes·HCl to give product **P1**. Pathway C is different from pathways A and B, in which NHC acts as a Brønsted acid/base catalyst. First, the NHC acts as a base to abstract the α-hydrogen of **1** and thus make the α-carbon atom in **C1** a nucleophile, which could then conduct a nucleophilic attack on the chalcone forming intermediate **C2**. The intramolecular cyclization of **C2** leads to intermediate **B6**, which could then abstract a hydrogen from the protonated NHC to generate the final product **P1**. Because no intermediate can be detected in experiments, it is still very difficult to understand thoroughly the detailed reaction mechanisms as well as the chemoselectivity.

Over the past two decades, DFT has been demonstrated to be a powerful method for clarifying the detailed reaction mechanisms and predicting the stereoselectivities as well as chemoselectivities with high accuracy in organocatalytic reactions.[22−32] It is worth mentioning that because of the special reactivities and broad applications of the NHC-catalyzed reactions, they also have attracted much attention from theoretical chemists.[33−58] In particular, NHC-catalyzed annulation of enals with chalcone giving access to enolate-type lactone and cyclopentene compounds has been theoretically studied by us and the Domingo group, respectively.[40,47] It turned out that the reaction leading to enolate-type lactone and cyclopentene

DOI: 10.1021/acs.joc.5b01222
J. Org. Chem. 2015, 80, 8619−8630

Scheme 5. Free Energy Profile of Reaction Pathway A for NHC-Catalyzed Annulation of Allenals with Chalcone Leading to P1

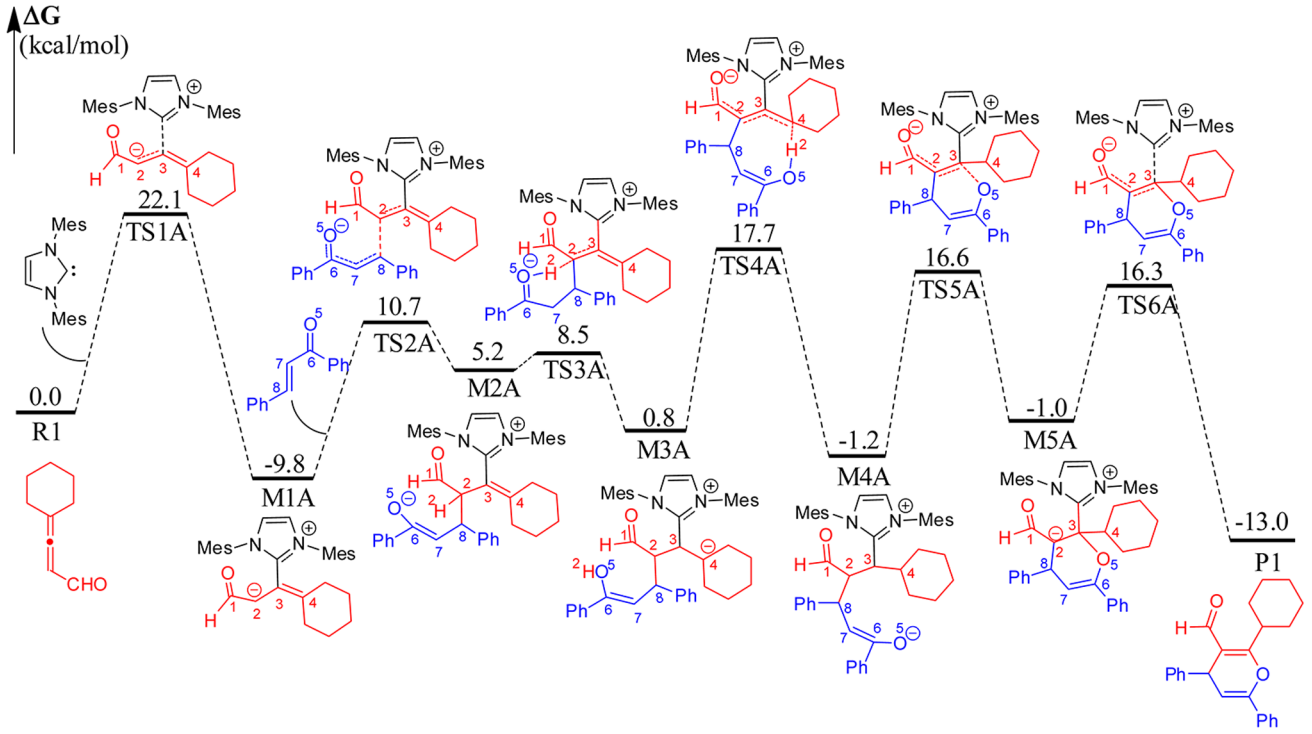

compounds proceeds following two different reaction pathways involving homoenolate and enolate intermediates depicted in Scheme 1b, respectively.[47,59] These theoretical studies have greatly enhanced our understanding of the mechanistic insights into the NHC catalytic processes and the roles of NHCs in the reaction course. Our interest in NHC-catalyzed reactions prompts us to investigate this domino process in detail. Moreover, to explain the observed chemoselectivity, we think it is necessary to take the homoenolate and enolate pathways (pathways D and E involving Breslow intermediate **D1**) leading to products **P2** and **P3** shown in Scheme 4 into consideration.

It is worth mentioning that when we were preparing the manuscript, a related paper was published by Yang et al.[60] In their work, they investigated the three possible reaction pathways (pathways A−C) shown in Scheme 3 leading to the polysubstituted pyranyl aldehydes as well as the homoenolate pathway D leading to cyclopentene by using a simplified model NHC catalyst. They raised two key points in their paper. First, pathway A leading to the formation of polysubstituted pyranyl aldehydes is the most energetically favorable, in agreement with the experimental observation that **P1** is the main product. Second, the rate-determining step in pathway A is the addition of the conjugate to the central carbon atom of the allene moiety with an activation free energy of 25.8 kcal/mol (Figure 1), while the formation of Breslow intermediate **D2** requires an activation energy of 59.5 kcal/mol, which indicates that the reaction process is kinetically disfavorable and thus homoenolate pathway D is impossible.

However, upon closer inspection of the free energy profile shown in Figure 1, it became clear that there are some problems in their conclusions. First, on the basis of the Cutin−Hammett principle,[61] the overall energy barrier for a catalytic cycle should be the energy difference between the lowest and the highest stationary points on the energy profile. Therefore, the energy barrier for preferred pathway A should be the energy difference between **a1** and **TSa4**, i.e., ΔG = 31.3 kcal/mol but not 25.8 kcal/mol (Figure 1). The energy barrier of 31.3 kcal/mol is slightly higher because the reaction can proceed smoothly at room temperature. Thus, their computations fail to correlate with experimental observations. This failure might be caused by their use of the highly simplified model catalyst, in which the two crucial Mes group attached to N were replaced with methyl groups. The simplified model lost the originally present steric repulsion and weak binding interactions between the reactant and catalyst and thus may have a significant influence on the obtained results.[62] Second, it has been demonstrated many times that protic solvent or acid/base can assist in the formation of the Breslow intermediate and lower the energy barrier significantly.[40,47,57] However, in Yang's paper, they suggested that the formation of the Breslow intermediate go through a three-membered transition state and thus is kinetically disfavorable. Thus, we think this conclusion has a problem, and the key factor determining the observed chemoselectivity is not identified correctly by them. In addition, they did not consider the enolate pathway depicted in Scheme 4, and thus, their computation is incomplete. Given the shortcomings of the previous investigation, an exhaustive computational effort is indispensable for clarifying the detailed reaction mechanism as well as the chemoselectivity.

In the study presented here, a DFT theoretical investigation toward the title reaction was pursued to shed light on details of each elementary step at the molecular level and to reach a more comprehensive understanding of the chemoselectivity of this interesting catalytic annulation. This computational work extends the scope of that earlier work by using the model reaction shown in Schemes 3 and 4.

COMPUTATIONAL DETAILS

All theoretical calculations were performed using the Gaussian 09[63] suite of programs. The geometrical structures of all the stationary points in

DOI: 10.1021/acs.joc.5b01222
J. Org. Chem. 2015, 80, 8619−8630

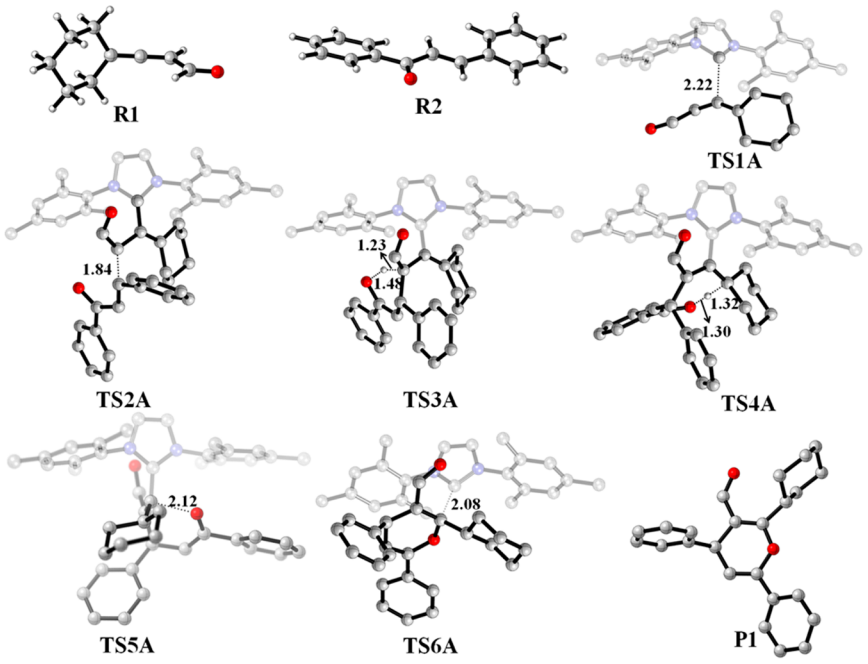

Figure 2. Optimized reactant, transition state, and product structures associated with pathway A. The distances are shown in angstroms. The hydrogens not involved in the reaction have been omitted. The NHC catalyst is rendered transparent for the sake of clarity.

Scheme 6. Free Energy Profile of Reaction Pathway B for NHC-Catalyzed Annulation of Allenals with Chalcone Leading to P1

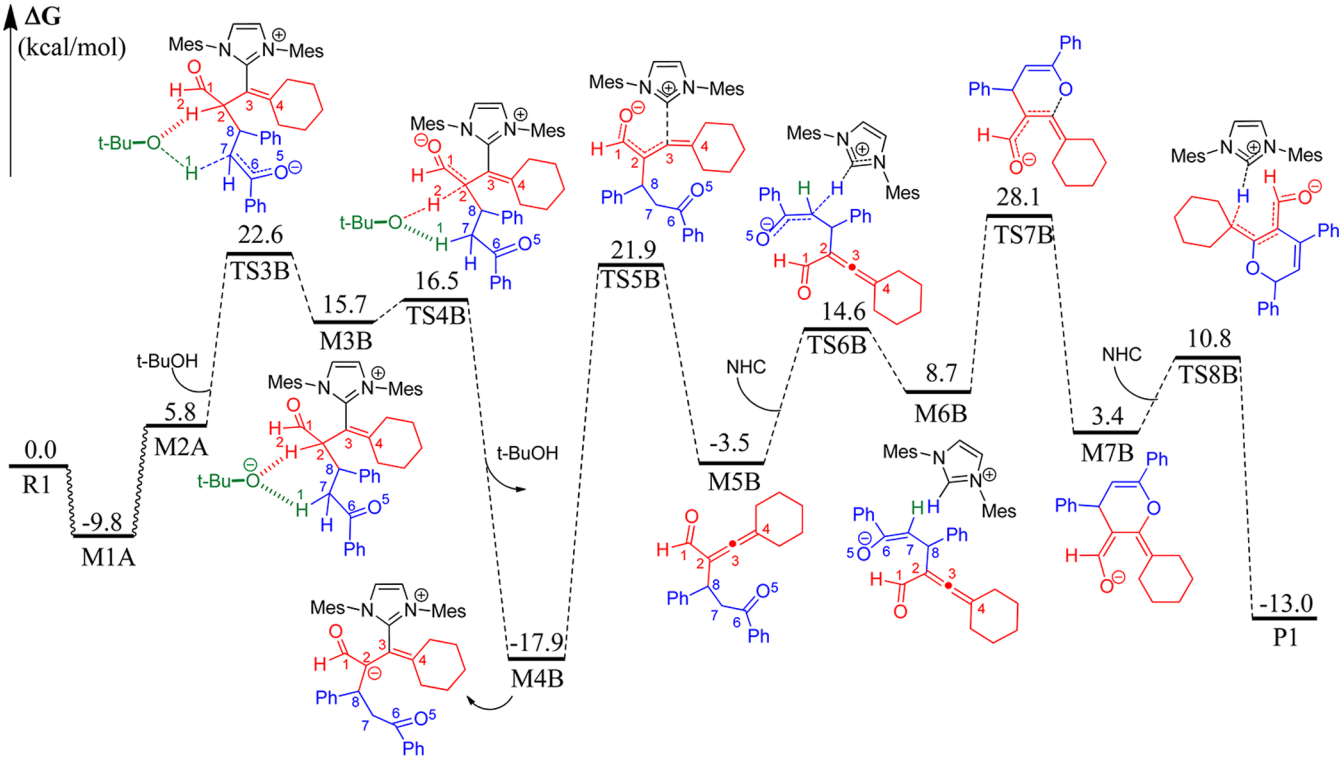

the energy profiles were optimized at the B3LYP/6-31G(d,p) level[64,65] in the gas phase. The Berny algorithm was employed for both minimizations and optimizations to transition states.[66] The corresponding vibrational frequencies were calculated at the same level to take into account the zero-point vibrational energy (ZPE) and to identify whether the structure is a transition state or a minimum. We confirmed that all reactants and intermediates had no imaginary frequencies, and each transition state had only one imaginary frequency. Intrinsic reaction coordinate (IRC) calculations,[67,68] at the same level of theory, were performed to ensure that the transition states led to the expected reactants and products. We then refined the energy by performing single-point energy calculations at the M06-2X/6-311++G(d,p) level[69−71] based on the B3LYP/6-31G(d,p) optimized structures in solvent tetrahydrofuran using the IEFPCM solvent model.[72,73] In the following discussion, the energies obtained by addition of thermal correction at the B3LYP/6-31G(d,p) level to the corresponding single energy at the M06-2X/6-311++G(d,p) level in the solvent are used.

DOI: 10.1021/acs.joc.5b01222
J. Org. Chem. 2015, 80, 8619−8630

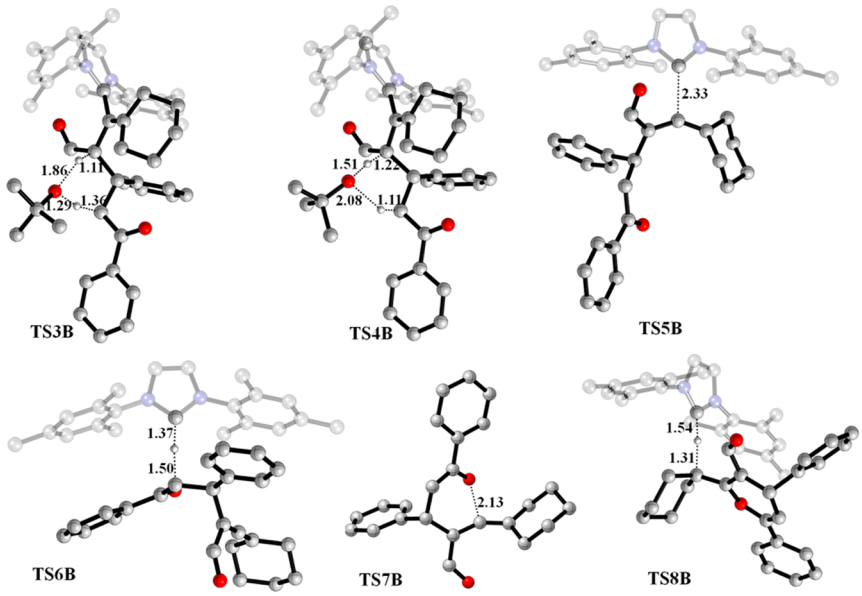

Figure 3. Optimized transition state structures associated with pathway B. The distances are shown in angstroms. The hydrogens not involved in the reaction have been omitted. The NHC catalyst is rendered transparent for the sake of clarity.

RESULTS AND DISCUSSION

Reaction Mechanisms. In this study, multiple possible reaction pathways (shown in Schemes 5−9) for the title reaction were thoroughly investigated through DFT calculations. They include the NHC-catalyzed reaction pathways (A−C) producing polysubstituted pyranyl aldehyde **P1**, pathway D leading to cyclopentene product **P2**, and pathway E for formation of enolate-type lactone **P3**. Detailed insights into the different reaction pathways are discussed in the following sections.

NHC-Catalyzed Annulation Pathways A and B. In pathway A, NHC initiates the reaction by nucleophilic attack on the positively charged center carbon atom of allenyl, i.e., the C3 atom. This reaction process is accomplished via transition state **TS1A** and generates intermediate **M1A**, in which the α-carbon, i.e., C2 atom, is rendered negative. The energy barrier for this step amounts to 22.1 kcal/mol, and the energy of generated **M1A** is 9.8 kcal/mol lower than that of **R1+NHC**, indicating that this reaction process is highly exergonic and irreversible. Next, the negatively charged C2 atom of **M1A** can nucleophilically attack the β-carbon of chalcone **R2** (i.e., C8 atom) via transition state **TS2A** leading into intermediate **M2A**. This step requires an activation energy of 20.5 kcal/mol, and the formed intermediate **M2A** is 5.2 kcal/mol higher than **R1+R2+NHC**, indicating that **M2A** is unstable. During this reaction process, the length of the C2−C8 forming bond changes from 1.84 Å in **TS2A** to 1.60 Å in **M2A** (as shown in Figure 2). As suggested by Ma et al., intermediate **M2A** should then isomerize to **M4A** (shown in Scheme 5). Direct isomerization should go through a four-membered ring (H2−C2−C3−C4) transition state, which is impossible because of the strong strain. Herein, we suggest that **M2A** isomerizes to **M4A** via two consecutive proton transfer processes. Specifically, the negative oxygen atom O5 can first abstract H2 attached with C2 via the seven-membered ring transition state **TS3A** affording intermediate **M3A**. As shown in Scheme 5, the energy barrier for this step is only 3.3 kcal/mol as a consequence of the developed negative charge on the O5 atom. Accompanied by the hydrogen transfer from C2 to O5, the negative charge gradually accumulates on the C4 atom. This facilitates the subsequent hydrogen transfer from O5 to C4, which is accomplished via an eight-membered ring transition state **TS4A** with an energy barrier of 16.9 kcal/mol. Then, intramolecular cyclization via C3−O5 bond formation affords intermediate **M5A**. During this process, the C3−O5 bond distance changes from 2.12 Å in **TS5A** to 1.48 Å in **M5A**, indicating that the C3−O5 bond is gradually formed in **M5A**. The energy barrier for this single step amounts to 17.8 kcal/mol, not a high barrier at room temperature. Followed by the intramolecular cyclization is the extrusion of NHC catalyst and product formation via transition state **TS6A**. The energy barrier of 17.3 kcal/mol indicates that NHC is not a bad leaving group. As shown, the energy barrier for the entire pathway A should be the energy difference between the lowest stationary point, **M1A**, and the highest stationary point, **TS4A** (ΔG = 27.5 kcal/mol). The optimized transition state structures are shown in Figure 2.

Pathway B and pathway A diverge from intermediate **M2A**. In pathway B (shown in Scheme 6), intermediate **M2A** does not isomerize to **M4A** but to **M4B**; i.e., H2 is not transferred to C4 but to C7. Similarly, direct hydrogen transfer from C2 to C7 is not feasible because of the strong strain associated with the four-membered ring transition state, because the reaction system contains small amounts of *t*-BuOH and protic solvent has been demonstrated to be able to assist the proton transfer process in many reactions.[74−78] Herein, we proposed that *t*-BuOH can assist the hydrogen transfer from C2 to C7. According to our calculated results, the *t*-BuOH-mediated hydrogen transfer process is stepwise. At first, *t*-BuOH transfers its hydroxyl hydrogen H1 to C7 via transition state **TS3B** and affords intermediate **M3B**, in which the hydroxyl oxygen is hydrogen bonded with both H1 and H2 (Figure 3). Next, the deprotonated *t*-BuO$^-$ would abstract the H2 attached to C2 giving rise to intermediate **M4B**. The free energy barrier for *t*-BuOH-assisted hydrogen transfer amounts to 32.4 kcal/mol (from **M1A** to **TS3B**), indicating that this reaction process is not energetically favored. Then, the elimination of NHC from **M4B** affords intermediate **M5B**, with an activation free energy of 39.8 kcal/mol. In the following, NHC would act as a Brønsted base to abstract the α-hydrogen attached to C7 leading to intermediate **M6B**. The following intramolecular cyclization via transition

DOI: 10.1021/acs.joc.5b01222
J. Org. Chem. 2015, 80, 8619−8630

state **TS7B** results in intermediate **M7B**. The activation free energy for **TS7B** amounts to 46.0 kcal/mol with respect to the lowest stationary point, **M4B**. Finally, the protonation of **M7B** by IMes·HCl via transition state **TS8B** produces product **P1** and regenerates the NHC catalyst. As shown from the free energy profile, the free energy barrier for pathway B was calculated to be as high as 46.0 kcal/mol, associated with the cyclization step, indicating that pathway B is not energetically favorable.

Brønsted Acid/Base-Catalyzed Annulation Pathway C. In the experimental work, it was envisioned that NHC may act as a Brønsted base to initiate the reaction. Therefore, we also took this possibility into consideration. According to the calculated results, this possible reaction pathway (i.e., pathway C) consists of four reaction steps. NHC first acts as a Brønsted base to deprotonate the α-hydrogen of allenyl **R1** giving rise to the negatively charged intermediate **M1C** via transition state **TS1C**, which then goes through 1,4-addition with chalcone to form intermediate **M2C** via transition state **TS1C** (Figure 4). The

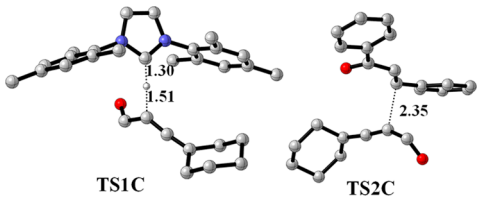

Figure 4. Optimized transition state structures associated with pathway C. The distances are shown in angstroms. The hydrogens not involved in the reaction have been omitted. The NHC catalyst is rendered transparent for the sake of clarity.

subsequent reaction steps proceed following pathway B and thus are not discussed. According to the free energy profile shown in Scheme 7, the rate-limiting step for pathway C is the second step with the highest free energy barrier of 39.1 kcal/mol, indicating that pathway C is also not energetically favorable.

NHC-Catalyzed Homoenolate Pathway D. To investigate why the reaction does not yield cyclopentene product **P2**, we also explored the possible reaction pathway D for chemoselective formation of cyclopentene product **P2**. It is noteworthy that the chemoselective formation of cyclopentene product **P2** involves the Breslow intermediate. As shown in Scheme 8, NHC initially nucleophilically attacks the carbonyl carbon of allenals **R1** via transition state **TS1D** (Figure 5) leading to intermediate **M1D**. This step requires an activation energy of 16.7 kcal/mol and is endergonic with the obtained intermediate **M1D** 8.9 kcal/mol higher in energy than **NHC+R1**, indicating that this reaction process is easily reversible. The subsequent proton transfer from carbonyl carbon to carbonyl oxygen affords Breslow intermediate **M2D**. The direct 1,2-migration mechanism via a three-membered ring transition state requires an activation energy as high as 56.1 kcal/mol (data not shown), indicating that its occurrence is impossible. Alternatively, our calculated results indicate that *t*-BuOH can mediate the proton transfer process in this step and can significantly reduce the energy barrier to 28.5 kcal/mol, demonstrating that formation of the Breslow intermediate is kinetically possible. Homoenolate intermediate **M2D** would then nucleophilically attack α,β-unsaturated chalcone **R2** to yield the enol−enolate **M3D**. This step involves two events: C3−C8 bond formation and proton transfer from O1 to O5 occur simultaneously. The activation energy for **TS3D** was calculated to be 35.9 kcal/mol, and generated intermediate **M3D** is 9.4 kcal/mol higher than the reactant. Following the formation of **M3D** is the keto−enol tautomerization producing intermediate **M4D**, and *t*-BuOH was also proven to be able to assist the proton transfer process in this step. The energy barrier for **TS4D** amounts to 34.8 kcal/mol with respect to **R1+R2+NHC+*t*-BuOH**. The generation of intermediate **M4D** is irreversible with an energy barrier of 41.9 kcal/mol for the reverse reaction. Then, intermediate **M4D** would experience an intramolecular aldolic addition via transition state **TS5D** to form intermediate **M5D**, which can then convert into bicyclic ether **M6D**. The activation free energies associated with the aldolic addition step and bicyclic ether formation step amount to 20.5 and 25.4 kcal/mol, respectively. The subsequent elimination of NHC requires an activation energy of only 5.1 kcal/mol. At last, intermediate **M7D** experiences an extrusion of a molecule of carbon dioxide via transition state **TS8D** affording cyclopentene product **P2**, and the energy barrier for this step was calculated to

Scheme 7. Free Energy Profile of Reaction Pathway C for NHC-Catalyzed Annulation of Allenals with Chalcone Leading to P1

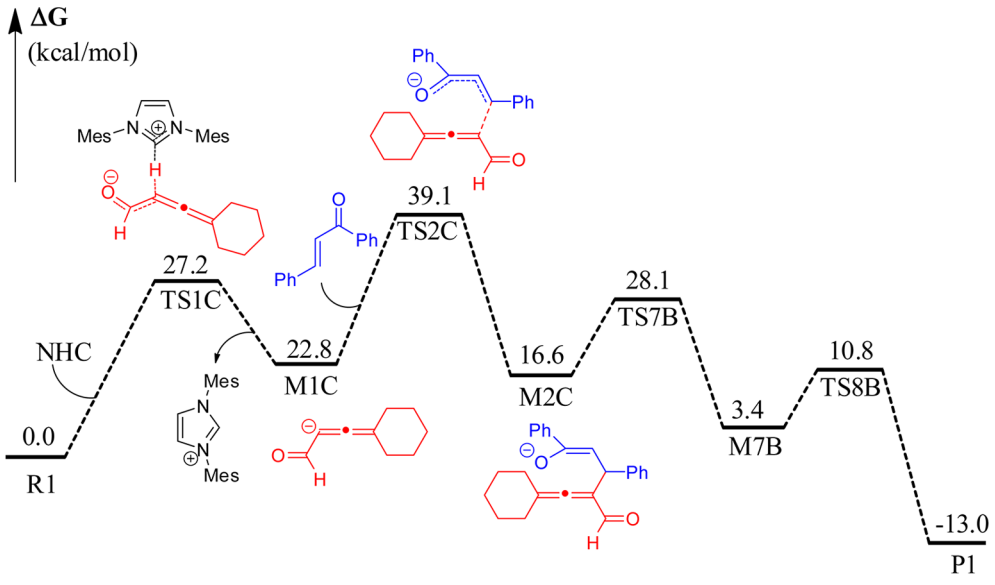

DOI: 10.1021/acs.joc.5b01222
J. Org. Chem. 2015, 80, 8619−8630

Scheme 8. Free Energy Profile of Reaction Pathway D for NHC-Catalyzed Annulation of Allenals with Chalcone Leading to P2

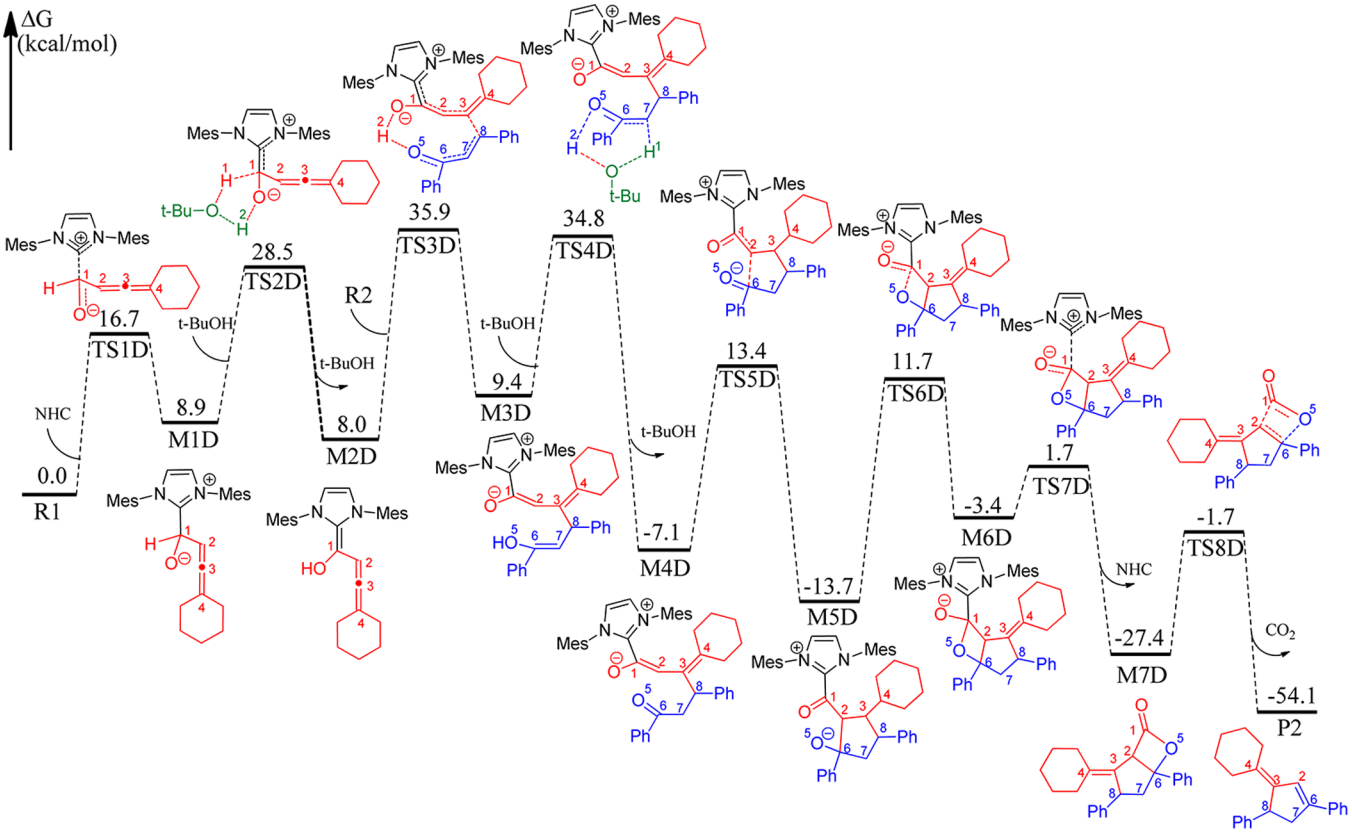

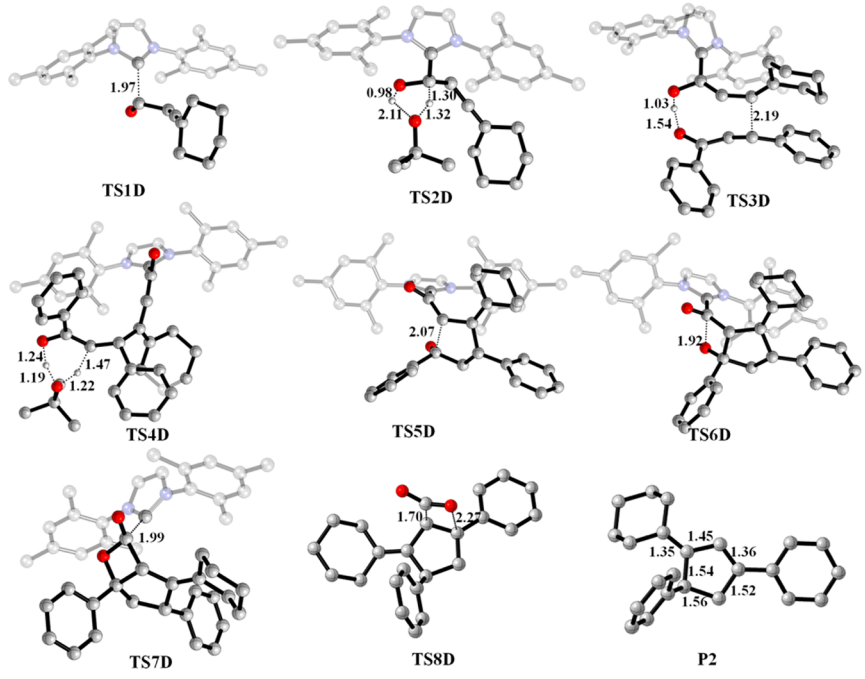

Figure 5. Optimized transition state structures associated with pathway D. The distances are shown in angstroms. The hydrogens not involved in the reaction have been omitted. The NHC catalyst is rendered transparent for the sake of clarity.

be 25.7 kcal/mol. On the whole, the energy barrier for the entire pathway is 35.9 kcal/mol associated with **TS3D**.

NHC-Catalyzed Enolate Pathway E. NHC-catalyzed [4+2] annulations of enals with chalcones leading to enolate-type lactone products also involve Breslow intermediate **M2D**. In this pathway, **M2D** would convert to **M3E** via a hydrogen shift from the hydroxyl oxygen to the *β*-carbon, i.e., C3 atom. The calculated results reveal that *t*-BuOH can also mediate this proton transfer process through transition state **TS3E** (Figure 6) and generate enolate intermediate **M3E**, which can then react

DOI: 10.1021/acs.joc.5b01222
J. Org. Chem. 2015, 80, 8619−8630

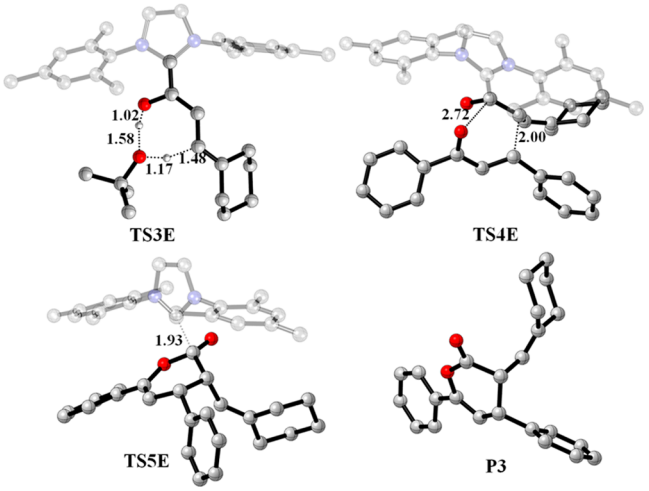

Figure 6. Optimized transition state structures and product **P3** associated with pathway E. The distances are shown in angstroms. The hydrogens not involved in the reaction have been omitted. The NHC catalyst is rendered transparent for the sake of clarity.

with chalcone via [4+2] cycloaddition. The free energy barrier for **TS3E** was calculated to be 17.7 kcal/mol (Scheme 9). The following [4+2] cycloaddition of **M3E** with chalcone proceeds concertedly via transition state **TS4E** with an activation free energy barrier of 19.5 kcal/mol. Generated intermediate **M4E** can then eliminate the NHC catalyst easily via transition state **TS5E** and yield enolate-type lactone product **P3**. On the whole, the enolate pathway leading to product **P3** comprises five steps, and the energy barrier for the whole reaction pathway is 28.5 kcal/mol associated with formation of Breslow intermediate **M2D**.

Further Analysis of the Chemoselectivity. By now, the five possible reaction pathways of the title reaction have been discussed in detail. In summary, the free energy barriers for pathways A–E are 27.5, 46.0, 39.1, 35.9, and 28.5 kcal/mol, respectively. Apparently, reaction pathway A is the most energetically favorable, which is in agreement with the experimental results that show that **P1** is the only observed product. An interesting aspect for pathways D and E is that both of them involve Breslow intermediate **M2D**, which is formed via nucleophilic addition of NHC to the carbonyl carbon atom of allenals followed by a *t*-BuOH-assisted proton transfer. Remarkably, the formation of the Breslow intermediate requires an activation free energy of 28.5 kcal/mol (associated with **TS2D**), and the reaction process is endergonic by 8.0 kcal/mol, indicating that the reaction process is easily reversible (shown in Scheme 8), while in pathway A, the reaction process does not involve the Breslow intermediate. Instead, NHC initiates the reaction by nucleophilic attack on the center carbon atom of allenals and produces intermediate **M1A**. The corresponding activation energy barrier for **TS1A** was calculated to be 22.1 kcal/mol, and the generation of **M1A** was found to be exergonic by 9.8 kcal/mol, indicating that the reverse reaction with an activation free energy of 31.9 kcal/mol is impossible (shown in Scheme 5). Therefore, although the highest free energy barrier for pathway E is only 1.0 kcal/mol higher than that of pathway A, enolate-type product **P3** cannot be obtained because formation of Breslow intermediate **M2D** is thermodynamically more disfavored than formation of intermediate **M1A**. This conclusion is very different from that of Yang, in which formation of the Breslow intermediate requires an activation energy as high as 59.5 kcal/

Scheme 9. Free Energy Profile of Reaction Pathway E for NHC-Catalyzed Annulation of Allenals with Chalcone Leading to P3

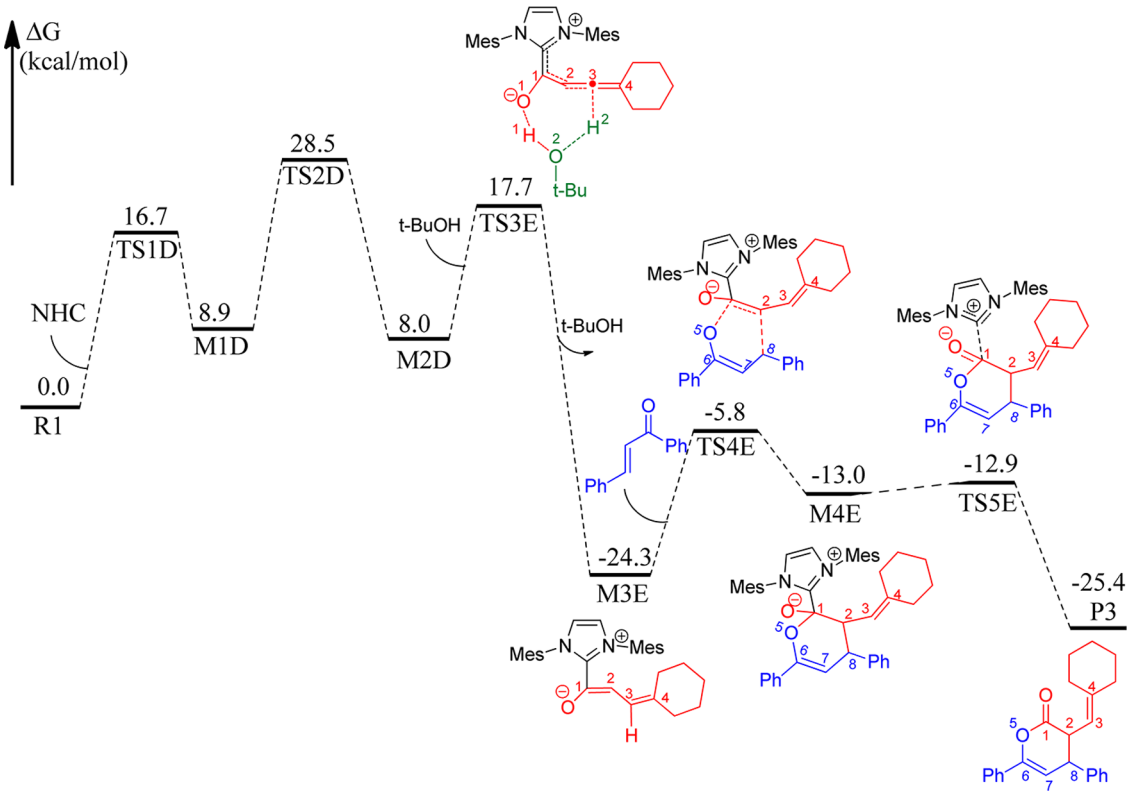

DOI: 10.1021/acs.joc.5b01222
J. Org. Chem. 2015, 80, 8619–8630

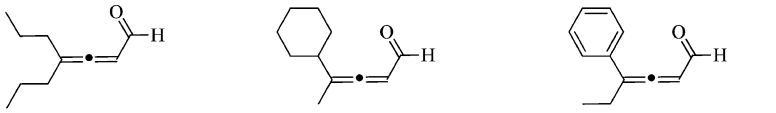

Figure 7. Calculated free energy difference between **M1A1** and **M2D1** for **R11**, **M1A2** and **M2D2** for **R12**, and **M1A3** and **M2D3** for **R13**.

mol, the result being that this reaction process is kinetically unfavorable. In summary, we can conclude that the highly exergonic nucleophilic attack (i.e., thermodynamically stable intermediate **M1A**) and the facile subsequent steps (proton transfer, cyclization, and catalyst regeneration) in pathway A result in its feasibility.

On the basis of our results and discussions, we conclude that the observed chemoselectivity is thermodynamically controlled but not kinetically controlled. It can be predicted that if the energy of Breslow intermediate **M2D** is significantly higher than that of **M1A** (e.g., >15.0 kcal/mol), the homoenolate and enolate pathway would not occur. To verify this assumption, we selected three other reaction models in the experimental report, in which the substituent groups on **R1** were changed, and compared the corresponding intermediate energies for **M1A** and **M2D**. The calculated results (shown in Figure 7) reveal that in all the three cases, Breslow intermediate **M2D** is much more unstable than **M1A**, in agreement with the experimentally observed chemoselectivities.

To compare our calculated results with Yang's "truncated model" at the same level, we also performed calculations for the stationary points in the key pathways at the M06-2X/6-311++G(d,p)//M06-2X/6-31G(d,p) level. All the results and discussions are given in the Supporting Information.

CONCLUSION

In this study, the detailed reaction mechanisms as well as the chemoselectivity for the NHC-catalyzed annulation of allenals with chalcones were investigated. Multiple possible reaction pathways (A–E) leading to three possible products were taken into consideration. Our calculated results indicate that pathway A leading to the polysubstituted pyranyl aldehydes is most energetically favored, and the energy barrier for the entire catalytic process is 27.5 kcal/mol. In contrast to the limited investigation by Yang's group, our calculated results can more reasonably explain the experimental observations, demonstrating that selection of the appropriate catalyst model is of great importance.

The NHC in the reaction system has been identified as being responsible for the activation of allenals toward its reaction with chalcone. The lower energy barrier of pathway A relative to pathways B and C reveals that NHC cannot be just viewed as a Brønsted base but instead should be viewed as a Lewis base (nucleophile), which can enhance the nucleophilicity of allenals. Furthermore, the comparison of pathway A with pathways D and E determined that the chemoselective formation of polysubstituted pyranyl aldehydes is caused by the exergonic characteristic of the first reaction process associated with the nucleophilic addition of NHC to the central carbon of allenals in pathway A and the low-energy barriers of the subsequent reaction steps. Specifically, this pathway comprises six reaction steps: nucleophilic attack of NHC on allenals, followed by 1,4-addition to chalcone, two consecutive intramolecular proton transfers, intramolecular cycloaddition, and dissociation of the NHC catalyst.

We proposed that the observed chemoselectivity is thermodynamically but not kinetically controlled, and if the Breslow intermediate is significantly unstable compared to the other possible intermediate, the occurrence of the homoenolate and enolate pathways would be impossible. Further calculations of the different reaction models support this point, which may provide valuable clues for predicting the chemoselective outcome of this kind of reaction.

ASSOCIATED CONTENT

Supporting Information

The Supporting Information is available free of charge on the ACS Publications website at DOI: 10.1021/acs.joc.5b01222.

Calculated energies for the stationary points in the key pathways at the M06-2X/6-311++G(d,p)//M06-2X/6-31G(d,p) level; Cartesian coordinates and ZPE (zero-point energy), E (electronic energy), E_0 (sum of electronic and zero-point energies), H (sum of electronic and thermal enthalpies), and G (sum of electronic and thermal free energies) values of the reactants, intermediates, transition states, and products obtained at the B3LYP/6-31G(d,p) level; and single-point energies of all reported structures at M06-2X/6-311++G(d,p) level in solvent THF using the IEFPCM model (PDF)

AUTHOR INFORMATION

Corresponding Authors

*E-mail: donghuiwei@zzu.edu.cn.
*E-mail: changjunbiao@zzu.edu.cn.

Notes

The authors declare no competing financial interest.

ACKNOWLEDGMENTS

This work was supported financially by the National Natural Science Foundation of China (21303167 and 21403199), the China Postdoctoral Science Foundation (2013M530340 and 2014M552010), and the Zhengzhou University Scientific Research Foundation (1411316003).

REFERENCES

(1) Bugaut, X.; Glorius, F. *Chem. Soc. Rev.* **2012**, *41*, 3511.
(2) Biju, A. T.; Kuhl, N.; Glorius, F. *Acc. Chem. Res.* **2011**, *44*, 1182.
(3) Enders, D.; Niemeier, O.; Henseler, A. *Chem. Rev.* **2007**, *107*, 5606.
(4) Nair, V.; Menon, R. S.; Biju, A. T.; Sinu, C. R.; Paul, R. R.; Jose, A.; Sreekumar, V. *Chem. Soc. Rev.* **2011**, *40*, 5336.
(5) Hopkinson, M. N.; Richter, C.; Schedler, M.; Glorius, F. *Nature* **2014**, *510*, 485.
(6) Flanigan, D. M.; Romanov-Michailidis, F.; White, N. A.; Rovis, T. *Chem. Rev.* **2015**, DOI: 10.1021/acs.chemrev.5b00060.

DOI: 10.1021/acs.joc.5b01222
J. Org. Chem. 2015, 80, 8619–8630

(7) Breslow, R. *J. Am. Chem. Soc.* **1958**, *80*, 3719.
(8) Stetter, H. *Angew. Chem.* **1976**, *88*, 695.
(9) Burstein, C.; Glorius, F. *Angew. Chem., Int. Ed.* **2004**, *43*, 6205.
(10) Sohn, S. S.; Rosen, E. L.; Bode, J. W. *J. Am. Chem. Soc.* **2004**, *126*, 14370.
(11) He, M.; Struble, J. R.; Bode, J. W. *J. Am. Chem. Soc.* **2006**, *128*, 8418.
(12) Nair, V.; Babu, B. P.; Vellalath, S.; Suresh, E. *Chem. Commun.* **2008**, 747.
(13) Nair, V.; Vellalath, S.; Babu, B. P.; Varghese, V.; Paul, R. R.; Suresh, E. *Org. Biomol. Chem.* **2010**, *8*, 4861.
(14) Nair, V.; Vellalath, S.; Poonoth, M.; Mohan, R.; Suresh, E. *Org. Lett.* **2006**, *8*, 507.
(15) Nair, V.; Poonoth, M.; Vellalath, S.; Suresh, E.; Thirumalai, R. *J. Org. Chem.* **2006**, *71*, 8964.
(16) Nair, V.; Vellalath, S.; Poonoth, M.; Suresh, E. *J. Am. Chem. Soc.* **2006**, *128*, 8736.
(17) Nair, V.; Babu, B. P.; Vellalath, S.; Varghese, V.; Raveendran, A. E.; Suresh, E. *Org. Lett.* **2009**, *11*, 2507.
(18) Fang, X.; Chen, X.; Lv, H.; Chi, Y. R. *Angew. Chem., Int. Ed.* **2011**, *50*, 11782.
(19) White, N. A.; DiRocco, D. A.; Rovis, T. *J. Am. Chem. Soc.* **2013**, *135*, 8504.
(20) Fu, Z.; Sun, H.; Chen, S.; Tiwari, B.; Li, G.; Robin Chi, Y. *Chem. Commun.* **2013**, *49*, 261.
(21) Ma, D. K.; Qiu, Y. A.; Dai, J. X.; Fu, C. L.; Ma, S. M. *Org. Lett.* **2014**, *16*, 4742.
(22) Cheong, P. H.-Y.; Legault, C. Y.; Um, J. M.; Çelebi-Ölçüm, N.; Houk, K. N. *Chem. Rev.* **2011**, *111*, 5042.
(23) Mustard, T. J. L.; Mack, D. J.; Njardarson, J. T.; Cheong, P. H.-Y. *J. Am. Chem. Soc.* **2013**, *135*, 1471.
(24) Pattawong, O.; Mustard, T. J. L.; Johnston, R. C.; Cheong, P. H.-Y. *Angew. Chem., Int. Ed.* **2013**, *52*, 1420.
(25) McIntosh, M. L.; Johnston, R. C.; Pattawong, O.; Ashburn, B. O.; Naffziger, M. R.; Cheong, P. H.-Y.; Carter, R. G. *J. Org. Chem.* **2012**, *77*, 1101.
(26) Pierce, M. D.; Johnston, R. C.; Mahapatra, S.; Yang, H.; Carter, R. G.; Ha-Yeon Cheong, P. *J. Am. Chem. Soc.* **2012**, *134*, 13624.
(27) McGarraugh, P. G.; Johnston, R. C.; Martínez-Muñoz, A.; Cheong, P. H.-Y.; Brenner-Moyer, S. E. *Chem. - Eur. J.* **2012**, *18*, 10742.
(28) Hong, X.; Liu, P.; Houk, K. N. *J. Am. Chem. Soc.* **2013**, *135*, 1456.
(29) McMahon, T. C.; Medina, J. M.; Yang, Y.-F.; Simmons, B. J.; Houk, K. N.; Garg, N. K. *J. Am. Chem. Soc.* **2015**, *137*, 4082.
(30) Lam, Y.-h.; Houk, K. N. *J. Am. Chem. Soc.* **2015**, *137*, 2116.
(31) Cheng, G.-J.; Zhang, X.; Chung, L. W.; Xu, L.; Wu, Y.-D. *J. Am. Chem. Soc.* **2015**, *137*, 1706.
(32) Xu, L.; Hilton, M. J.; Zhang, X.; Norrby, P.-O.; Wu, Y.-D.; Sigman, M. S.; Wiest, O. *J. Am. Chem. Soc.* **2014**, *136*, 1960.
(33) Langdon, S. M.; Legault, C. Y.; Gravel, M. *J. Org. Chem.* **2015**, *80*, 3597.
(34) Xie, H.; Zhao, L.; Yang, L.; Lei, Q.; Fang, W.; Xiong, C. *J. Org. Chem.* **2014**, *79*, 4517.
(35) Munz, D.; Strassner, T. *Chem. - Eur. J.* **2014**, *20*, 14872.
(36) Katayev, D.; Larionov, E.; Nakanishi, M.; Besnard, C.; Kündig, E. P. *Chem. - Eur. J.* **2014**, *20*, 15021.
(37) Allolio, C.; Strassner, T. *J. Org. Chem.* **2014**, *79*, 12096.
(38) Domingo, L. R.; Saez, J. A.; Arno, M. *Org. Biomol. Chem.* **2014**, *12*, 895.
(39) Domingo, L. R.; Zaragoza, R. J.; Saez, J. A.; Arno, M. *Molecules* **2012**, *17*, 1335.
(40) Domingo, L. R.; Zaragoza, R. J.; Arno, M. *Org. Biomol. Chem.* **2010**, *8*, 4884.
(41) Domingo, L. R.; Zaragoza, R. J.; Arno, M. *Org. Biomol. Chem.* **2011**, *9*, 6616.
(42) Zhao, L.; Chen, X. Y.; Ye, S.; Wang, Z.-X. *J. Org. Chem.* **2011**, *76*, 2733.
(43) Huang, F.; Lu, G.; Zhao, L.; Li, H.; Wang, Z.-X. *J. Am. Chem. Soc.* **2010**, *132*, 12388.
(44) Wei, D. H.; Zhu, Y. Y.; Zhang, C.; Sun, D. Z.; Zhang, W. J.; Tang, M. S. *J. Mol. Catal. A: Chem.* **2011**, *334*, 108.
(45) Zhang, W. J.; Zhu, Y. Y.; Wei, D. H.; Li, Y. X.; Tang, M. S. *J. Org. Chem.* **2012**, *77*, 10729.
(46) Zhang, W. J.; Wei, D. H.; Tang, M. S. *J. Org. Chem.* **2013**, *78*, 11849.
(47) Li, Z. Y.; Wei, D. H.; Wang, Y.; Zhu, Y. Y.; Tang, M. S. *J. Org. Chem.* **2014**, *79*, 3069.
(48) Li, Y.; Zhu, Y.; Zhang, W.; Wei, D.; Ran, Y.; Zhao, Q.; Tang, M. *Phys. Chem. Chem. Phys.* **2014**, *16*, 20001.
(49) Zhang, M. M.; Wei, D. H.; Wang, Y.; Li, S. J.; Liu, J. F.; Zhu, Y. Y.; Tang, M. S. *Org. Biomol. Chem.* **2014**, *12*, 6374.
(50) Wang, Y.; Ren, J. Y.; Qi, S. J.; Wei, D. H.; Tang, M. S. *Comput. Theor. Chem.* **2014**, *1049*, 35.
(51) Wang, Y.; Zheng, L.; Wei, D.; Tang, M. *Org. Chem. Front.* **2015**, *2*, 874.
(52) Kuniyil, R.; Sunoj, R. B. *Org. Lett.* **2013**, *15*, 5040.
(53) Verma, P.; Verma, P.; Sunoj, R. B. *Org. Biomol. Chem.* **2014**, *12*, 2176.
(54) Reddi, Y.; Sunoj, R. B. *Org. Lett.* **2012**, *14*, 2810.
(55) Verma, P.; Patni, P. A.; Sunoj, R. B. *J. Org. Chem.* **2011**, *76*, 5606.
(56) Reddi, Y.; Sunoj, R. B. *ACS Catal.* **2015**, *5*, 1596.
(57) Zhang, Q.; Yu, H.-Z.; Fu, Y. *Org. Chem. Front.* **2014**, *1*, 614.
(58) Jang, K. P.; Hutson, G. E.; Johnston, R. C.; McCusker, E. O.; Cheong, P. H. Y.; Scheidt, K. A. *J. Am. Chem. Soc.* **2014**, *136*, 76.
(59) Domingo, L. R.; Zaragoza, R. J.; Arno, M. *Org. Biomol. Chem.* **2010**, *8*, 4884.
(60) Wei, X.; Fang, R.; Yang, L. *Catal. Sci. Technol.* **2015**, *5*, 3352.
(61) Kozuch, S.; Shaik, S. *Acc. Chem. Res.* **2011**, *44*, 101.
(62) Paddon-Row, M. N.; Anderson, C. D.; Houk, K. N. *J. Org. Chem.* **2009**, *74*, 861.
(63) Frisch, M. J.; Trucks, G. W.; Schlegel, H. B.; Scuseria, G. E.; Robb, M. A.; Cheeseman, J. R.; Montgomery, J. A., Jr.; Vreven, T.; Udin, K. N.; Burant, J. C.; Millam, J. M.; Yengar, S. S.; Tomasi, J.; Barone, V.; Mennucci, B.; Cossi, M.; Scalmani, G.; Rega, N.; Petersson, G. A.; Nakatsuji, H.; Hada, M.; Ehara, M.; Toyota, K.; Fukuda, R.; Hasegawa, J.; Shida, M.; Nakajima, T.; Honda, Y.; Kitao, O.; Nakai, H.; Klene, M.; Li, X.; Knox, J. E.; Hratchian, H. P.; Cross, J. B.; Bakken, V.; Adamo, C.; Jaramillo, J.; Gomperts, R.; Stratmann, R. E.; Yazyev, O.; Austin, A. J.; Cammi, R.; Pomelli, C.; Ochterski, J. W.; Ayala, P. Y.; Morokuma, K.; Voth, G. A.; Salvador, P.; Dannenberg, J. J.; Zakrzewski, V. G.; Dapprich, S.; Daniels, A. D.; Strain, M. C.; Farkas, O.; Malick, D. K.; Rabuck, A. D.; Raghavachari, K.; Foresman, J. B.; Ortiz, J. V.; Cui, Q.; Baboul, A. G.; Clifford, S.; Cioslowski, J.; Stefanov, B. B.; Liu, G.; Liashenko, A.; Piskorz, P.; Komaromi, I.; Martin, R. L.; Fox, D. J.; Keith, T.; Al-Laham, M. A.; Peng, C. Y.; Nanayakkara, A.; Challacombe, M.; Gill, P. M. W.; Johnson, B.; Chen, W.; Wong, M. W.; Gonzalez, C.; Pople, J. A. *Gaussian 09*, revision A.02; Gaussian, Inc.: Wallingford, CT, 2009.
(64) Becke, A. D. *J. Chem. Phys.* **1993**, *98*, 5648.
(65) Lee, C.; Yang, W.; Parr, R. G. *Phys. Rev. B: Condens. Matter Mater. Phys.* **1988**, *37*, 785.
(66) Li, X. S.; Frisch, M. J. *J. Chem. Theory Comput.* **2006**, *2*, 835.
(67) Gonzalez, C.; Schlegel, H. B. *J. Chem. Phys.* **1989**, *90*, 2154.
(68) Gonzalez, C.; Schlegel, H. B. *J. Phys. Chem.* **1990**, *94*, 5523.
(69) Zhao, Y.; Truhlar, D. G. *Theor. Chem. Acc.* **2008**, *120*, 215.
(70) Zhao, Y.; Truhlar, D. G. *J. Chem. Theory Comput.* **2008**, *4*, 1849.
(71) Zhao, Y.; Truhlar, D. G. *Acc. Chem. Res.* **2008**, *41*, 157.
(72) Sang-Aroon, W.; Ruangpornvisuti, V. *Int. J. Quantum Chem.* **2008**, *108*, 1181.
(73) Tomasi, J.; Mennucci, B.; Cancès, E. *J. Mol. Struct.: THEOCHEM* **1999**, *464*, 211.
(74) Cheng, B.; Huang, G.; Xu, L.; Xia, Y. *Org. Biomol. Chem.* **2012**, *10*, 4417.
(75) Huang, G.; Cheng, B.; Xu, L.; Li, Y.; Xia, Y. *Chem. - Eur. J.* **2012**, *18*, 5401.
(76) Xia, Y. Z.; Liang, Y.; Chen, Y. Y.; Wang, M.; Jiao, L.; Huang, F.; Liu, S.; Li, Y. H.; Yu, Z. X. *J. Am. Chem. Soc.* **2007**, *129*, 3470.
(77) Shi, F. Q.; Li, X.; Xia, Y.; Zhang, L.; Yu, Z. X. *J. Am. Chem. Soc.* **2007**, *129*, 15503.

DOI: 10.1021/acs.joc.5b01222
J. Org. Chem. 2015, 80, 8619−8630

(78) Qiao, Y.; Chang, J.; Zheng, L.; Lu, M. *Org. Biomol. Chem.* **2015**, *13*, 7558.

DOI: 10.1021/acs.joc.5b01222
J. Org. Chem. 2015, 80, 8619−8630